



# The multifaceted role of GCM1 during trophoblast differentiation in the human placenta

Mariyan J. Jeyarajah<sup>a</sup> , Gargi Jaju Bhattad<sup>a</sup> , Rachel D. Kelly<sup>b</sup> , Kelly J. Baines<sup>a</sup> , Adam Jaremek<sup>a</sup> , Fei-Hung P. Yang<sup>a</sup>, Hiroaki Okae<sup>c</sup>, Takahiro Arima<sup>c</sup>, Vanessa Dumeaux<sup>a,d,e</sup> , and Stephen J. Renaud<sup>a,f,1</sup>

Edited by Janet Rossant, Gairdner Foundation, Toronto, Canada; received February 20, 2022; accepted October 14, 2022

Remodeling of the uterine vasculature by invasive extravillous trophoblasts (EVTs) is a critical aspect of human placentation. Insufficient EVT invasion can lead to severe obstetrical complications like preeclampsia, intrauterine growth restriction, and preterm birth. Glial cells missing-1 (GCM1) is a transcription factor that is crucial for proper placentation in mice, and is highly expressed in human syncytiotrophoblast (ST) and EVT. GCM1 is classically considered a master regulator of ST formation, but little is known about its contribution to the development and function of EVTs. Therefore, in this study we test the hypothesis that GCM1 is a critical regulator of both EVT and ST development and function. We show that GCM1 is highly expressed in human trophoblast stem (TS) cells differentiated into either ST or EVTs. Knockdown of GCM1 in TS cells hindered differentiation into both ST and EVT pathways. When placed in ST media, GCM1-knockdown cells formed small, unstable clusters; when placed in EVT media, cells had altered morphology and transcript profiles resembling cells trapped in an intermediate state between CT and EVT, and invasive capacity through matrix was reduced. RNA sequencing analysis of GCM1-deficient TS cells revealed downregulation of EVT-associated genes and enrichment in transcripts related to WNT signaling, which was linked to decreased expression of the EVT master regulator ASCL2 and the WNT antagonist NOTUM. Our findings reveal an essential role of GCM1 during ST and EVT development, and suggest that GCM1 regulates differentiation of human TS cells into EVTs by inducing expression of ASCL2 and NOTUM.

pregnancy | placenta | trophoblast | differentiation | stem cells

The placenta is a remarkable structure that forms the primary interface between maternal and fetal tissues. To facilitate normal fetal growth and development, the placenta must permit maternal–fetal transfer of nutrients and gases while simultaneously preventing passage of substances that can harm the fetus (1). The epithelial cells responsible for establishing the placental architecture are called trophoblasts, and they perform critical functions to support fetal development and stimulate maternal physiological adaptations required for pregnancy. There are several trophoblast sublineages with unique morphologies and specialized functions that contribute to anatomically distinct regions of the placenta. These trophoblast sublineages arise from trophoblast stem (TS) cells through a multilineage differentiation pathway (1, 2).

In humans, progenitor cells known as cytotrophoblasts (CTs) line the placental epithelium and are capable of self-renewal or bipotential differentiation along syncytiotrophoblast (ST) or extravillous trophoblast (EVT) pathways. ST is a unique entity comprised of billions of nuclei contained within a single interconnected cytoplasm, which bathes in maternal blood and serves as the primary site of maternal–fetal nutrient and gas exchange. ST is formed and continuously replenished by CTs differentiating and fusing into it (3, 4). On the other hand, CTs located at the tips of large villi near the utero–placental junction are fated to form EVTs. Proximally, EVTs proliferate as stratified cell columns; distally, EVTs develop invasive properties and migrate into the decidua up to the inner third of the myometrium (5). Invasive EVTs intercalate into and remodel various uterine structures, notably spiral arteries, causing these vessels to transform into low-resistance, high-capacity conduits capable of delivering a consistent supply of maternal blood to the placenta to support sustenance of the rapidly growing fetus during the second half of pregnancy (6). Failure of EVTs to remodel spiral arteries can result in placental insufficiency and serious pregnancy complications such as preeclampsia, intrauterine growth restriction, and stillbirth (7, 8).

Insights into trophoblast lineage development have often emanated from mouse studies in which TS cell culture protocols have been well characterized for decades. While there are some similarities in placental organization between mice and humans, there are also major differences in the placental structure and composition including restricted depth of trophoblast invasion in the former and extensive invasion in the latter, suggesting the likelihood

## Significance

Proper placental development is critical for pregnancy success. Placental maldevelopment is linked with serious pregnancy complications that jeopardize the health of both mother and child. The parenchymal cells of the placenta are trophoblasts, which arise from trophoblast stem cells differentiating through one of two distinct lineage pathways: syncytiotrophoblast, which regulates maternal-fetal nutrient transfer, and extravillous trophoblasts (EVTs), which remodel the uterine vasculature. Glial cells missing-1 (GCM1) is a transcription factor classically associated with syncytiotrophoblast formation, but GCM1 is also expressed in EVTs. In this study, human trophoblast stem cells were used to corroborate the role of GCM1 in syncytiotrophoblast formation and uncover its critical role in EVT development. We conclude that GCM1 contributes to multiple aspects of human placentation.

Author contributions: M.J.J. and S.J.R. designed research; M.J.J., G.J.B., K.J.B., and F.-H.P.Y. performed research; H.O. and T.A. contributed new reagents/analytic tools; M.J.J., R.D.K., A.J., V.D., and S.J.R. analyzed data; and M.J.J. and S.J.R. wrote the paper.

The authors declare no competing interest.

This article is a PNAS Direct Submission.

Copyright © 2022 the Author(s). Published by PNAS. This article is distributed under Creative Commons Attribution-NonCommercial-NoDerivatives License 4.0 (CC BY-NC-ND).

<sup>1</sup>To whom correspondence may be addressed. Email: srenaud4@uwo.ca.

This article contains supporting information online at <https://www.pnas.org/lookup/suppl/doi:10.1073/pnas.2203071119/-/DCSupplemental>.

Published November 28, 2022.

of both conserved and divergent regulatory pathways controlling mouse and human placentation (9). One such example of a regulatory factor that potentially exerts both conserved roles and functional disparities between mouse and human placentation is glial cells missing-1 (*GCM1*). In mice and humans, *GCM1* is a transcription factor that is expressed almost exclusively in the placenta (10–12). In mice, *GCM1* expression is restricted to the placental labyrinth (site of nutrient and gas exchange in rodents), where it regulates branching morphogenesis and ST formation (10). In humans, *GCM1* appears to have a similar role as a master regulator of ST formation (13). However, unlike the restricted expression patterns in mice, *GCM1* is also detectable in human EVT<sub>s</sub> (12–14). Thus, *GCM1* appears to have an additional, not well-characterized role in human EVT development and function. In this study, we used recently established human TS cells (15) to uncover the importance of *GCM1* for ST and EVT development, and identify the EVT master regulator *ASCL2* (16) and the WNT antagonist *NOTUM* (17) as downstream *GCM1* targets critical for the formation of EVT<sub>s</sub>. We conclude that *GCM1* is an indispensable regulator of both ST and EVT differentiation in the human placenta.

## Results

***GCM1* is Expressed in Human ST and EVT<sub>s</sub>.** To determine whether *GCM1* expression is altered during human TS cell differentiation, cells were cultured in CT stem state, or induced to form ST and EVT<sub>s</sub> (Fig. 1*A*). Successful differentiation to ST was determined by reduced expression of the CT marker *TEAD4* by 20-fold and increased expression of *CGB* by 580-fold. In cells cultured in EVT media, expression of *TEAD4* was decreased by 21-fold and the EVT marker *HLA-G* was increased 16-fold (Fig. 1*A* and *B*). Differentiation of CT<sub>s</sub> into ST and EVT<sub>s</sub> was associated with increased *GCM1* expression (10- and 15-fold increased expression in ST and EVT<sub>s</sub> compared with CT; Fig. 1*C–E*). Upregulation of *GCM1* in ST and EVT<sub>s</sub> was also confirmed in two other human TS cell clones derived from first trimester female (CT27) and male (CT29) placentas (*SI Appendix*, Fig. S1).

Next, to determine which cells at the maternal–fetal interface express *GCM1*, we analyzed publicly available single-cell RNA sequencing (RNAseq) data using cells isolated from early gestation placentas along with maternal blood and decidual cells (18). *GCM1* is almost exclusively expressed in ST and EVT<sub>s</sub>, and only sporadically expressed at low levels in CT<sub>s</sub> (*SI Appendix*, Fig. S2*A*). Analysis of another single-cell RNAseq dataset utilizing trophoblasts isolated from first trimester (6–12 wk) placentas (19) similarly shows that *GCM1* is highly expressed in precursor-ST (cluster 6; defined by high expression of *ERVFRD-1*, *ERVV-1*, and *SDCI*), column CT<sub>s</sub> (cluster 7; defined by high expression of *ITGA2* and *HLA-G*), and EVT<sub>s</sub> (cluster 8; defined by high expression of *ITGAI*, *ITGA5*, and *HLA-G*). *GCM1* expression was low in most CT populations (clusters 1–5; defined by high expression of *TEAD4* and *ELF5*), although some expression was detected in CT cluster 4, which likely represents a population of CT<sub>s</sub> transitioning to more differentiated phenotypes based on reduced expression of stem and proliferation markers such as *CCNA2*, *ITGA6*, and *TP63* (*SI Appendix*, Fig. S2*B–D*). Localization of *GCM1* in differentiated trophoblast lineages was further verified through in situ hybridization and immunohistochemistry using 7-wk human placenta. *GCM1* transcript and protein were readily detectable in ST (demarcated with immunohistochemistry for CGB) and EVT<sub>s</sub> (demarcated with immunohistochemistry for HLA-G; Fig. 1*F*). *GCM1* transcript was also detectable in several CT<sub>s</sub> as determined through in situ hybridization, consistent with expression patterns observed in single-cell RNAseq. However,

*GCM1* protein was rarely detected in CT<sub>s</sub>: only 3.7% of CT nuclei stained positive for *GCM1* protein. These cells seemed to be intermediately placed between CT and ST layers. In contrast, the majority of ST (CGB<sup>+</sup>) and EVT (HLA-G<sup>+</sup>) nuclei were positive for *GCM1* (*SI Appendix*, Fig. S2*E*). The different mRNA and protein localization of *GCM1* in the human placenta is consistent with another study (12) and likely relates to the extensive posttranslational modifications of *GCM1*, which confer stability to the protein (20). Overall, these data indicate that *GCM1* is expressed in differentiated trophoblasts of the human placenta.

### ***GCM1*-Deficient TS Cells Display Abrogated ST Differentiation.**

To confirm the role of *GCM1* in ST development, we infected human TS cells with lentivirus carrying control shRNAs or two distinct shRNAs targeting *GCM1* (*GCM1* KD1 and *GCM1* KD2). Compared with cells transduced with control shRNAs and cultured in ST media, *GCM1* mRNA and (more prominently) protein expression was reduced in cells transduced with *GCM1* KD1 and KD2 shRNAs (4.9- and 5.0-fold decreased protein expression in *GCM1* KD1 and KD2 ST, respectively, compared with control ST; *SI Appendix*, Fig. S3*A* and *B*). Differentiation of control cells into ST resulted in large, fused bodies with clear brush borders (*SI Appendix*, Fig. S3*C*). Conversely, *GCM1*-deficient cells placed in ST media lacked this morphology and appeared smaller in size (*SI Appendix*, Fig. S3*C*). Furthermore, expression of three distinct ST markers – *CGB*, *ERVFRD-1*, and *HSD11B2* – was profoundly down-regulated in *GCM1* KD1 and KD2 ST compared with control ST, despite a robust downregulation of the CT-associated gene *TEAD4* (*SI Appendix*, Fig. S3*D*). In stark contrast to control cells maintained in CT media, control ST cells did not express the tight junction protein *ZO-1* and strongly expressed CGB. *GCM1* KD1 and KD2 ST retained some *ZO-1* and although these cells expressed CGB, they were fewer in number and smaller in size when compared with control ST, indicating that *GCM1* may be important for ST integrity or stability (approximately 80% decreased fusion and 85% decreased ST area when comparing *GCM1* KD ST with control ST; *SI Appendix*, Fig. S3*E*). Since *GCM1* KD TS cells cultured in ST media produced small unstable ST clusters, we were unable to obtain sufficient high-quality materials for downstream analyses (e.g., low RIN values, poor cell viability), and therefore did not progress with further mechanistic analyses of these cells. Nonetheless, these data suggest that *GCM1*-deficiency in human TS cells results in poor ST development and stability.

**Impaired EVT Development in *GCM1*-Deficient TS Cells.** As the role of *GCM1* in EVT development is not well understood, our next step was to determine the importance of *GCM1* for EVT development and function. Human TS cells expressing control shRNAs exhibited 10-fold increased *GCM1* expression when differentiated toward EVT<sub>s</sub>. However, *GCM1* KD1 and KD2 cells exhibited reduced *GCM1* mRNA and protein expression when placed in EVT media (3.5- and 3.3-fold decreased protein expression compared with control EVT<sub>s</sub>, respectively; Fig. 2*A* and *B*). *GCM1* knockdown resulted in poor EVT differentiation, as observed through lack of mesenchymal spindle-shaped morphology (Fig. 2*C*). Additionally, compared with control EVT<sub>s</sub>, *GCM1* KD1 and KD2 had increased expression of *TEAD4* and decreased expression of three well-established EVT markers: *HLA-G*, *ITGAI*, and *MMP2* (Fig. 2*D*). Trophoblast differentiation is associated with mitotic arrest, so we next tested the proliferative capacity of human TS cells cultured in CT and EVT conditions. When CT<sub>s</sub> were differentiated toward EVT<sub>s</sub>, 5-ethynyl-2'-deoxyuridine (EdU) incorporation was decreased by 2.3-fold, indicating that

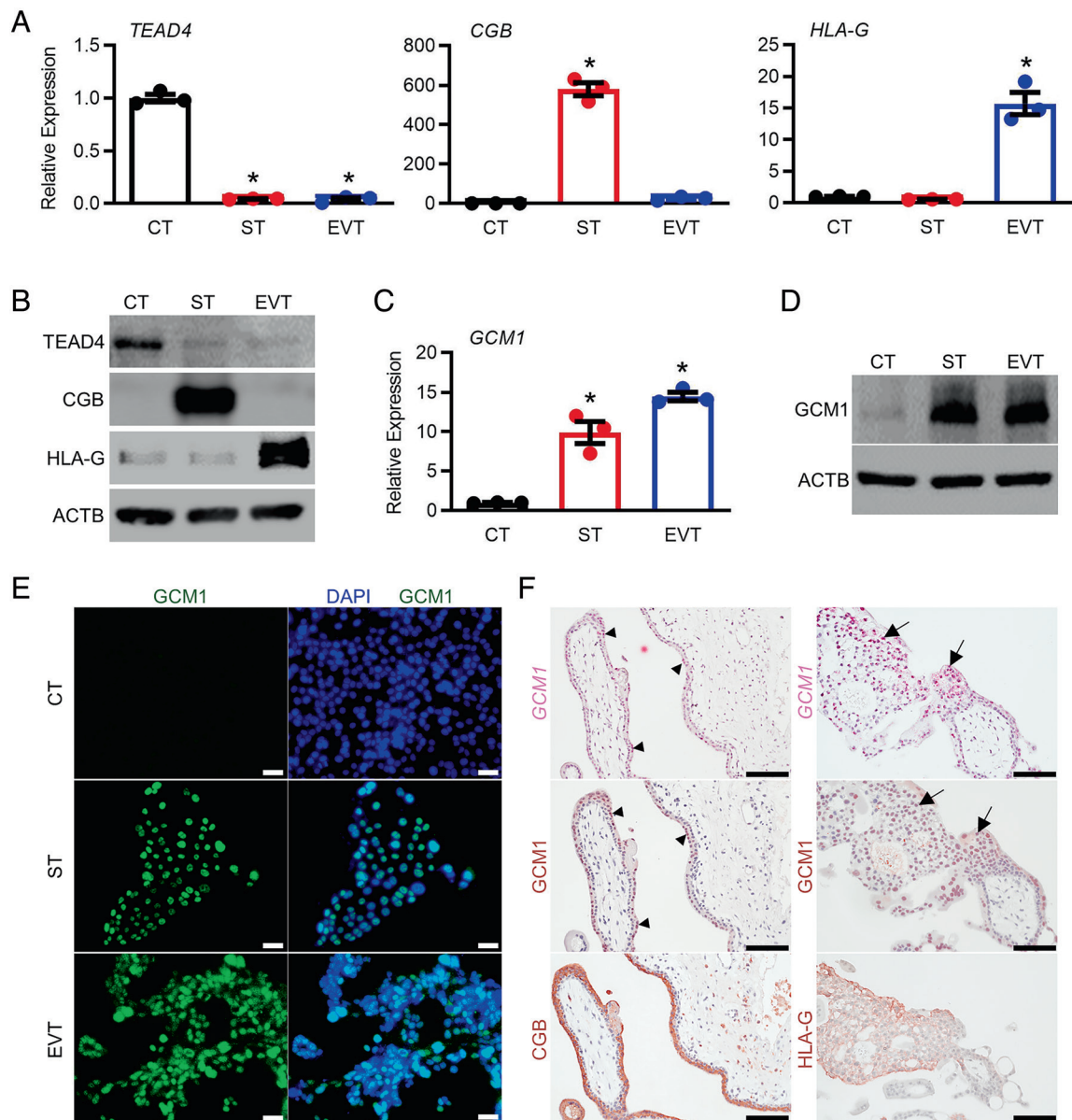


**Fig. 1.** GCM1 is expressed in human ST and EVTs. (A) Quantitative RT-PCR and (B) Western blot analysis of CT (*TEAD4*), ST (*CGB*), and EVT (*HLA-G*) markers in TS cells (CT30) maintained in CT stem state, or differentiated to ST or EVTs. (C) Quantitative RT-PCR, (D) Western blot and (E) immunofluorescence for *GCM1* (green) in TS cells in CT stem state, or differentiated to ST or EVTs. *ACTB* was used as a loading control for Western blotting. DAPI was used to demarcate nuclei. (F) In situ hybridization (pink dots) and immunohistochemistry (brown) for *GCM1* in 7-wk human placenta. Immunohistochemistry for *CGB* and *HLA-G* (brown) was used to demarcate ST and EVT, respectively. Arrowheads show *GCM1*-positive cells in the ST layer; arrows show representative EVTs positive for *GCM1*. Values significantly different from CT are indicated with an asterisk (\*,  $N = 3$ ,  $P < 0.05$ ). (Scale bar, 100  $\mu\text{m}$ .)

proliferation is inhibited in TS cells during differentiation toward EVTs (Fig. 2E). We found no difference in the proliferation capacity between control and *GCM1* KD TS cells either in CT stem state, or when differentiated into EVTs (Fig. 2E; only *GCM1* KD1 cells are shown). To recapitulate the invasive nature of EVTs in the placenta, a Matrigel-based invasion assay was performed. Both *GCM1* KD1 and KD2 EVTs exhibited reduced capacity to invade through Matrigel (2.2- and 1.8-fold decreased invasion through Matrigel compared with control EVTs; Fig. 2F). Overall, these results suggest that *GCM1* is required for EVT differentiation and consequently, *GCM1* knockdown cells have reduced invasive capacity.

**Gene Expression Analysis of *GCM1*-Deficient EVTs Reveals Impaired EVT Development.** To characterize global transcriptomic differences between control EVTs and *GCM1* KD EVTs, RNAseq was performed. Since similar results were obtained using *GCM1*

KD1 and KD2 cells in previous experiments, only KD1 cells were used for RNAseq analysis. A total of 21,914 transcripts were annotated. Principal component analysis showed that control and *GCM1* KD1 cells were closely related when cultured in the CT stem state (as expected, since *GCM1* levels are low in these cells), but when placed in EVT differentiation media, these two cell populations diverged (Fig. 2G). When comparing expression of all genes changed > two-fold between control CTs and EVTs (3,963 genes), *GCM1* KD1 EVTs showed some similarity in gene expression patterns with control EVTs since both are cultured in EVT media, but in general, the intensity of the increased and decreased gene expression patterns appeared blunted. Moreover, in some regions, *GCM1* KD1 EVTs had gene expression patterns consistent with cells maintained in the CT stem state. We conclude that *GCM1* KD1 EVTs have a transcriptional profile intermediate between control (and *GCM1* KD1) CTs and control EVTs,

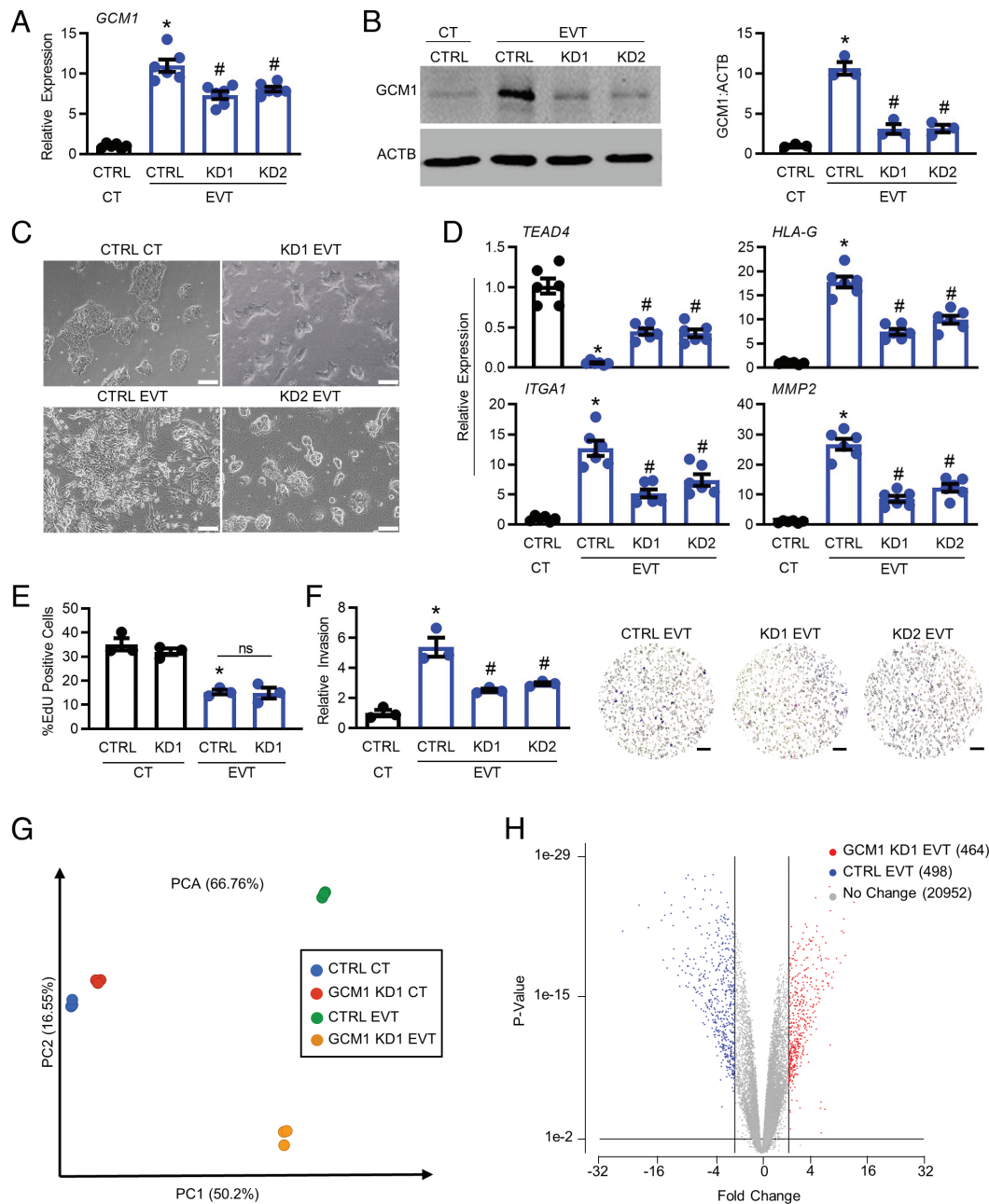


**Fig. 2.** GCM1 is required for EVT development. (A) Quantitative RT-PCR and (B) Western blot analysis showing GCM1 expression in control (CTRL) and two distinct GCM1 knockdown (KD1 and KD2) TS cells differentiated into EVTs. ACTB was used as a loading control for Western blotting. (C) Phase-contrast images depicting CTRL, GCM1 KD1, and GCM1 KD2 cells. (D) Quantitative RT-PCR analysis showing expression of one CT marker (*TEAD4*) and three EVT markers (*HLA-G*, *ITGA1*, and *MMP2*) in CTRL, GCM1 KD1, and GCM1 KD2 TS cells differentiated into EVTs. (E) Quantification of percent EdU-positive nuclei in CTRL and GCM1 KD1 TS cells in CT stem state, or differentiated into EVTs for 6 d. (F) Relative number of CTRL, GCM1 KD1, and GCM1 KD2 TS cells that invaded through Matrigel following differentiation into EVTs. Representative images of invaded cells are found to the right of the graph. Membrane pores are the black circles, cells are stained purple. (G) Principal component analysis showing relationship between replicates of CTRL and GCM1 KD1 cells cultured in CT or EVT media, using all expressed genes as input. Please note that CTRL and KD1 cells cluster close together in CT media, but diverge when cultured in EVT media. (H) Volcano plot showing the number of unique transcripts identified in RNAseq analysis. Transcripts up-regulated in GCM1 KD1 EVTs relative to CTRL EVTs are shown in red (fold change  $\geq 2$ ,  $P < 0.01$ ), and down-regulated transcripts are shown in blue. The X-axis represents magnitude of fold change, and the Y-axis shows the  $P$ -value. Values significantly different between CTRL CT and CTRL EVT are indicated with an asterisk (\*,  $P < 0.05$ ), and values significantly different between CTRL EVT and GCM1 KD1 EVT are indicated with a number sign (#,  $P < 0.05$ ); ns = not statistically significant.  $N = 6$  for (A) and (D), all other panels are  $N = 3$ . (Scale bar, 100  $\mu\text{m}$ .)

suggesting that the capacity of GCM1 KD1 EVTs to undergo proper EVT development was hindered (SI Appendix, Fig S4A).

When comparing control EVTs with GCM1 KD1 EVTs, 962 transcripts were found to be differentially expressed (Dataset S1;  $\geq$  two-fold,  $P < 0.01$ ). Of these transcripts, 464 were increased in GCM1 KD1 EVTs and 498 were decreased (Fig. 2H). Numerous well-established EVT-associated genes showed decreased expression in GCM1 KD1 EVTs compared with control EVTs, including *PAPPA*, *NOTUM*, *ITGA1*, *TFPI*, *ADAM12*, *ANGPTL4*,

*ADAM19*, *MMP2*, *FNI*, *ASCL2*, and *MMP15*. GCM1 KD1 EVTs (like CTs) also showed elevated expression of *TGFB2* and *CDX1*, which are factors associated with decreased trophoblast invasion, and increased expression of *ETS2* and *TP63*, which are highly expressed in progenitor trophoblast populations. To validate our RNAseq results, we next performed quantitative RT-PCR on select genes (e.g., *TFPI*, *PAPPA*, *IFIT1*, *ADAM19*, and *GJA1*), and the fold changes observed were consistent with results obtained using RNAseq (SI Appendix, Fig S4B). KEGG pathway

analysis was then performed on gene lists consisting of up-regulated and down-regulated ( $\geq$  two-fold expression) genes in GCM1 KD1 EVT cells compared with control EVTs. Examples of terms associated with up-regulated genes include Hippo and WNT signaling, which are highly associated with the CT stem state, whereas terms associated with down-regulated genes include steroid biosynthesis and peroxisome proliferator-activated receptor (PPAR) signaling, which are related to EVT functions (SI Appendix, Fig. S4C). Overall, these data support that GCM1-deficiency abrogates EVT development and function.

**Induced GCM1 Expression Stimulates Precocious Differentiation of Human TS Cells.** Our findings indicate that GCM1 is required for the formation of ST and EVT lineages. Therefore, our next goal was to determine whether induction of GCM1 enhances the rate of trophoblast differentiation. To achieve this goal, we cloned *GCM1* into a cumate-inducible expression system, generated lentivirus, and transduced human TS cells to establish a stable line in which *GCM1* expression could be induced by adding the small molecule, cumate. A different population of cells was transduced with an empty vector as a control to ensure that cumate itself did not affect human TS cell viability or differentiation. When human TS cells transduced with the cumate-inducible *GCM1* expression system were exposed to 200 or 300  $\mu\text{g}/\text{mL}$  cumate, *GCM1* was induced by approximately six-fold. There was no change in *GCM1* expression in cells transduced with the control vector at any concentration of cumate, so 200  $\mu\text{g}/\text{mL}$  was selected as the optimal dose for the next set of experiments (SI Appendix, Fig. S5A). This dose of cumate did not noticeably alter the morphology or viability of human TS cells maintained in the CT state (SI Appendix, Fig. S5B). GCM1 protein levels were also increased by 5.1-fold in TS cells transduced with the cumate-inducible *GCM1* expression system (SI Appendix, Fig. S5C). Last, since GCM1 is a trophoblast growth-restricting gene that inhibits proliferation, we tested whether GCM1 expression results in decreased EdU incorporation when cells are placed in basal differentiation media (i.e., when growth factors critical for promoting the TS cell stem state are removed) (21). Induction of GCM1 caused a 2.1-fold decrease in EdU incorporation compared with cells not treated with cumate, indicating that GCM1 inhibits cell proliferation (SI Appendix, Fig. S5D).

To determine whether induced GCM1 expression enhanced the rate of ST formation, TS cells possessing the cumate-inducible GCM1 system were exposed to ST differentiation media with or without 200  $\mu\text{g}/\text{mL}$  cumate. Cells were analyzed on day 3 or day 6 of differentiation and compared with CTs. On day 3, *GCM1* expression was increased by approximately four-fold and nine-fold without and with cumate compared with CTs, respectively. The increased expression of *GCM1* in cumate-treated cells paralleled an increase in *CGB* and *ERVFRD-1*. However, by day 6 when endogenous levels of *GCM1* are high and ST formation is robust, there was no difference in *GCM1*, *CGB*, or *ERVFRD-1* expression between cumate-treated and nontreated cells (SI Appendix, Fig. S6A). At the protein level, GCM1 was increased by 2.2-fold between cumate-treated and nontreated cells on day 3 of ST differentiation, but there was no difference on day 6 when endogenous GCM1 levels are high. Although there was no difference in CGB detected using Western blotting on day 3 of differentiation between cumate-treated and nontreated cells, the number of fused cells was increased by 2.4-fold following induction of GCM1 (SI Appendix, Fig. S6 B and C). Therefore, we conclude that induced expression of GCM1 causes precocious ST differentiation.

We next determined the effect of induced GCM1 expression on EVT differentiation. TS cells possessing the cumate-inducible GCM1 system were exposed to EVT differentiation media with or

without 200  $\mu\text{g}/\text{mL}$  cumate. Cells were analyzed 3 or 6 d later and compared with CTs. In cells receiving cumate, the appearance of protrusions reminiscent of EVTs was apparent by 3 d (SI Appendix, Fig. S7A). Also on day 3, *GCM1* expression was increased in cells exposed to cumate (2.6-fold compared with cells not treated with cumate). Increased *GCM1* expression was associated with increased expression of EVT-associated genes *HLA-G* and *MMP2* by 3.5- and 6.7-fold, respectively. There was no difference in *GCM1*, *HLA-G*, or *MMP2* expression on day 6 of differentiation between cumate-treated and nontreated cells, likely due to high endogenous levels of these transcripts and robust EVT differentiation (SI Appendix, Fig. S7B). GCM1 and HLA-G were also increased at the protein level by 2.3- and 4.4-fold, respectively, on day 3 of EVT differentiation in cells treated with cumate, whereas there were no differences in GCM1 or HLA-G levels on day 6 of differentiation between cumate-treated and nontreated cells (SI Appendix, Fig. S7C). Collectively, these findings strongly suggest that increased GCM1 expression is sufficient to cause precocious EVT differentiation.

**GCM1 Is a Transcriptional Regulator of ASCL2.** Of the 498 down-regulated genes identified in GCM1 KD1 cells by RNAseq, one of the most robustly down-regulated was *ASCL2*, a transcription factor known to play crucial roles in placental junctional zone development in rodents and EVT development in humans (16, 22). Quantitative RT-PCR confirmed significant downregulation of *ASCL2* in GCM1 KD1 and KD2 EVTs (4.5- and 2.9-fold decreased expression compared with control EVTs, respectively; Fig. 3A), whereas increased GCM1 expression on day 3 of EVT differentiation using the cumate-inducible system increased *ASCL2* expression by 2.2-fold (SI Appendix, Fig. S7D). In situ hybridization confirmed *ASCL2* localization within EVTs (demarcated through immunohistochemistry for HLA-G) of 7-wk human placentas (Fig. 3B). Given the robust downregulation of *ASCL2* in GCM1 KD EVTs, we hypothesized that GCM1 may directly regulate *ASCL2* expression. Both *GCM1* and *ASCL2* were increased within 3 d of EVT differentiation and expression of both factors progressively increased over the course of an 8-d EVT differentiation protocol, suggesting that these factors may work in concert to regulate the development of EVTs (Fig. 3C). Increased expression of *ASCL2* was also confirmed in two other human TS cell clones as they were induced to differentiate toward EVTs (CT27 and CT29; SI Appendix, Fig. S1). In silico analysis of the *ASCL2* promoter revealed a GCM1 consensus-binding site (GCCCGCAT) 1,851 bp upstream of *ASCL2* (Fig. 3D). Chromatin immunoprecipitation (ChIP) followed by quantitative PCR performed on 3-d differentiated EVT lysates revealed binding of GCM1 to the *ASCL2* promoter (25-fold increased binding when compared with IgG-negative controls). *ERVW-1*, a well-established GCM1 target gene affiliated primarily with cell fusion in ST but that is also highly expressed in EVTs (23), was used as a positive control for GCM1 binding. Indeed, our RNAseq analysis showed 4.1-fold increased expression of *ERVW-1* in control EVTs compared with CTs, and expression was reduced by 2.1-fold in GCM1 KD1 cells, providing further evidence that *ERVW-1* is induced in EVTs and its promoter is a suitable positive control to assess GCM1 binding. An 87-bp product adjacent to the transcription start site of *GAPDH* that does not contain a GCM1 consensus-binding site was used as a negative control (Fig. 3D). These data suggest that GCM1 binds upstream of *ASCL2* and is a putative driver of *ASCL2* expression during EVT differentiation.

**ASCL2-Deficient TS Cells Display Abrogated EVT Differentiation.** It was recently reported that downregulating *ASCL2* expression in human TS cells impairs EVT development (16). To confirm

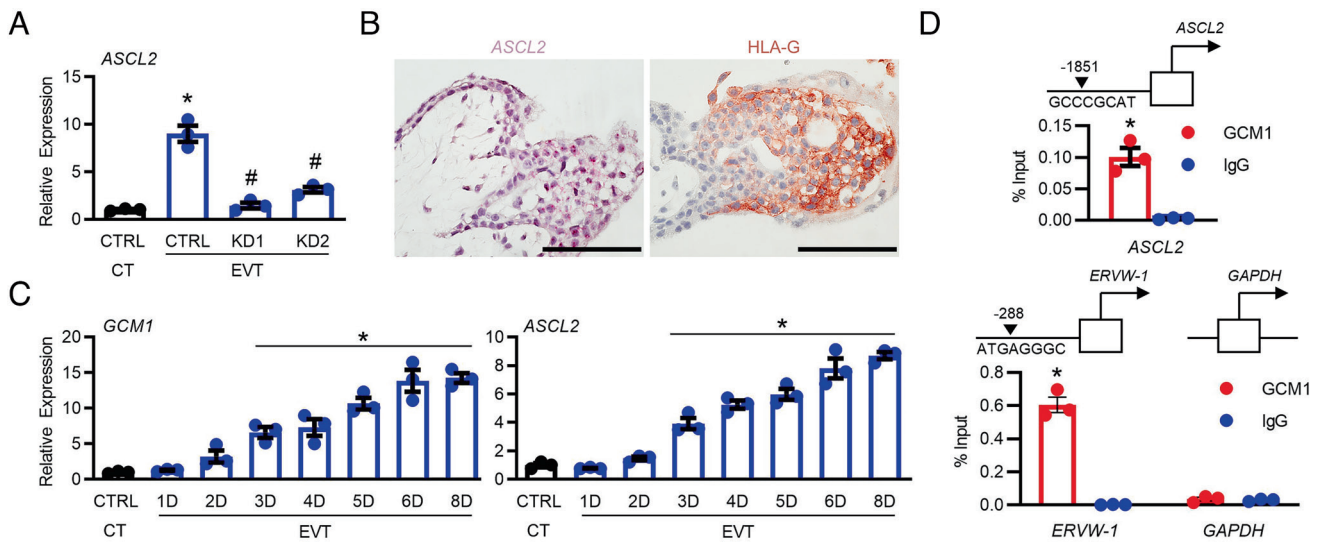


**Fig. 3.** GCM1 regulates *ASCL2* expression. (A) Quantitative RT-PCR analysis showing expression of *ASCL2* in control (CTRL) and GCM1 knockdown (KD1 and KD2) cells, differentiated to form EVTs. (B) In situ hybridization (pink dots) and immunohistochemistry (brown) for *ASCL2* and *HLA-G* in 7-wk human placenta, respectively. (C) Quantitative RT-PCR analysis showing *GCM1* and *ASCL2* expression in TS cells in CT stem state or placed in EVT media over an 8-d period. (D) ChIP was performed for GCM1 or IgG (negative control) in lysates of cells cultured in EVT media for 3 d, followed by quantitative PCR to detect enrichment 1,851 bp upstream of *ASCL2*. An established GCM1-binding site 288 bp upstream of *ERVV-1* was used as a positive control; an 87-bp product adjacent to the transcription start site of *GAPDH* that does not contain a GCM1 consensus-binding site was used as a negative control. In (A), values significantly different between CTRL CT and CTRL EVT are indicated with an asterisk (\*,  $N = 3$ ,  $P < 0.05$ ), and values significantly different between CTRL EVT and GCM1 KD EVT are indicated with a number sign (#,  $N = 3$ ,  $P < 0.05$ ). In (C), values significantly different from CT are shown using an asterisk (\*,  $N = 3$ ,  $P < 0.05$ ). In (D), statistical differences are shown using an asterisk (\*,  $N = 3$ ,  $P < 0.05$ ). (Scale bar, 100  $\mu$ m.)

these findings, a lentivirus-shRNA delivery strategy involving one control and two shRNAs targeting *ASCL2* (*ASCL2* KD1 and *ASCL2* KD2) was used, similar to the approach used to knockdown *GCM1* expression. Cells receiving *ASCL2* KD1 and KD2 shRNAs exhibited a 3.2- and 1.9-fold decrease in *ASCL2* expression, respectively, compared with cells receiving the control shRNA (*SI Appendix, Fig. S8A*). Cells with reduced *ASCL2* expression exhibited poor capacity to differentiate into EVTs, including an apparent lack of mesenchymal spindle-shaped morphology, which was similar to the phenotype observed in *GCM1* KD EVTs (*SI Appendix, Fig. S8B*). Furthermore, *ASCL2* KD1 and KD2 EVTs showed increased expression of *TEAD4* and decreased expression of EVT markers *HLA-G* and *ITGA1* (*SI Appendix Fig. S8C*). Consistent with the notion that *GCM1* acts upstream of *ASCL2*, there was no change in *GCM1* expression following knockdown of *ASCL2*. Cell proliferation was also unchanged (*SI Appendix, Fig. S8 C and D*; only *ASCL2* KD1 cells are shown in *D*). Last, similar to *GCM1*-deficient cells, *ASCL2* KD1 and KD2 EVTs exhibited a reduced capacity to invade Matrigel (2.1- and 1.8-fold decreased invasiveness compared with control EVTs; *SI Appendix, Fig. S8E*). Collectively, these results suggest that *ASCL2* plays a critical role in EVT development, and its deficiency leads to a similar phenotype as observed with *GCM1* KD EVTs.

**GCM1 and *ASCL2*-Deficiency Leads to Poor EVT Development in a Placental Spheroid Model.** To further characterize the role of *GCM1* and *ASCL2* in the development of EVTs, we created a placental spheroid model by culturing human TS cells in AggreWell 800 plates (*SI Appendix, Fig. S9A*). Once uniform spheroids were produced, they were transferred onto nonadherent plates and cultured either in CT or EVT media. In spheroids cultured in EVT media, *TEAD4* and *CGB* were down-regulated by 3.3- and 3.2-fold, while *HLA-G*, *ITGA1*, *GCM1*, and *ASCL2* were up-regulated by 3.7-, 4.7-, 2.9-, and 5.2-fold, respectively (*SI Appendix, Fig. S9B*). Similar results were obtained when evaluating protein levels, including decreased levels of *TEAD4* and *CGB* in spheroids

cultured in EVT media, and increased expression of *HLA-G* (*SI Appendix, Fig. S9C*). Furthermore, immunofluorescence revealed expression of cell junction markers *ZO-1* and *CDH1* in the center of all spheroids. *CGB* was localized to the outer perimeter of spheroids most prominently in CT conditions. Expression of *HLA-G* was detected only in spheroids cultured in EVT media (*SI Appendix, Fig. S9D*). Therefore, placental spheroids have the capacity to form multiple trophoblast lineages when cultured in defined medium conditions. We next tested the ability of *GCM1* and *ASCL2*-deficient TS cells to form EVTs when cultured as spheroids. As expected, spheroids generated from *GCM1* or *ASCL2*-deficient TS cells and cultured under EVT conditions showed poor development of EVTs including higher expression of *CDH1* and either low or undetectable expression of *HLA-G* (*SI Appendix, Fig. S9E*). These data further support a critical role of *GCM1* and *ASCL2* for EVT development.

**WNT Signaling is Up-Regulated in *GCM1*-Deficient EVTs.** Since WNT signaling was identified as one of the most up-regulated terms in *GCM1*-deficient EVTs, we further explored the possibility that *GCM1* promotes EVT formation by negatively regulating WNT signaling. RNAseq analysis revealed increased levels of several WNT-associated factors and down-regulated expression of the WNT suppressor *NOTUM* in *GCM1* KD1 EVTs (Fig. 4A). Immunofluorescence and quantitative RT-PCR further verified these findings: compared with control EVTs, expression of *NOTUM* was profoundly decreased in *GCM1* KD1 and KD2 EVTs by 10.6- and 14.7-fold, respectively (Fig. 4B and C). Conversely, increased *GCM1* expression on day 3 of EVT differentiation using the cumate-inducible system resulted in a 7.6-fold increase in *NOTUM* expression (*SI Appendix, Fig. S7E*). In silico analysis revealed a *GCM1* consensus-binding site (ATGCGGGC) 519 bp upstream of the *NOTUM*. Using ChIP followed by quantitative PCR, we found that *GCM1* binds to this site (Fig. 4D). Thus, *GCM1* may negatively regulate WNT signaling in human TS cells, at least in part, by inducing expression of *NOTUM*. To directly measure differences in WNT signaling activity between CTs and

EVTs, we performed a TOPFlash *Luciferase* reporter assay. The TOPFlash reporter carries TCF/LEF-binding sites upstream of firefly *Luciferase*, therefore the amount of luminescence serves as an indicator of  $\beta$ -catenin transcriptional activity and WNT signaling (24). *Luciferase* reporters carrying either wild-type or mutant TCF/LEF-binding sites were transfected into human TS cells cultured in CT and EVT conditions. Cells cultured in EVT conditions showed a 2.6-fold decrease in luminescence compared with cells cultured in CT conditions, indicating that  $\beta$ -catenin transcriptional activity is reduced during EVT differentiation (Fig. 4E). Cells transfected with the mutant reporter showed low levels of luminescence. We further evaluated levels of phosphorylated GSK3 $\beta$ (Tyr216), a negative regulator of WNT signaling (25). There was a 2.1-fold increase in pGSK3 $\beta$ (Tyr216) expression in control EVT cells when

compared with control CTs. GCM1 KD1 and KD2 EVT lysates showed 2.4- and 2.2-fold decreased expression, respectively, when compared with control EVT cells (Fig. 4F). Last, control and GCM1 KD EVT cells were transfected with *Luciferase* reporters carrying wild-type TCF/LEF-binding sites. Compared with control EVT cells, GCM1 KD1 and KD2 EVT cells showed increased luminescence (2.1- and 1.9-fold, respectively; Fig. 4G). These data suggest that GCM1 inhibits WNT/ $\beta$ -catenin activity during EVT differentiation.

**NOTUM Negatively Regulates WNT/ $\beta$ -Catenin Signaling and Promotes EVT Development.** Since GCM1 binds directly upstream of *NOTUM* and GCM1-deficient human TS cells exhibit decreased *NOTUM* expression and poor EVT differentiation, we next determined the role of NOTUM during

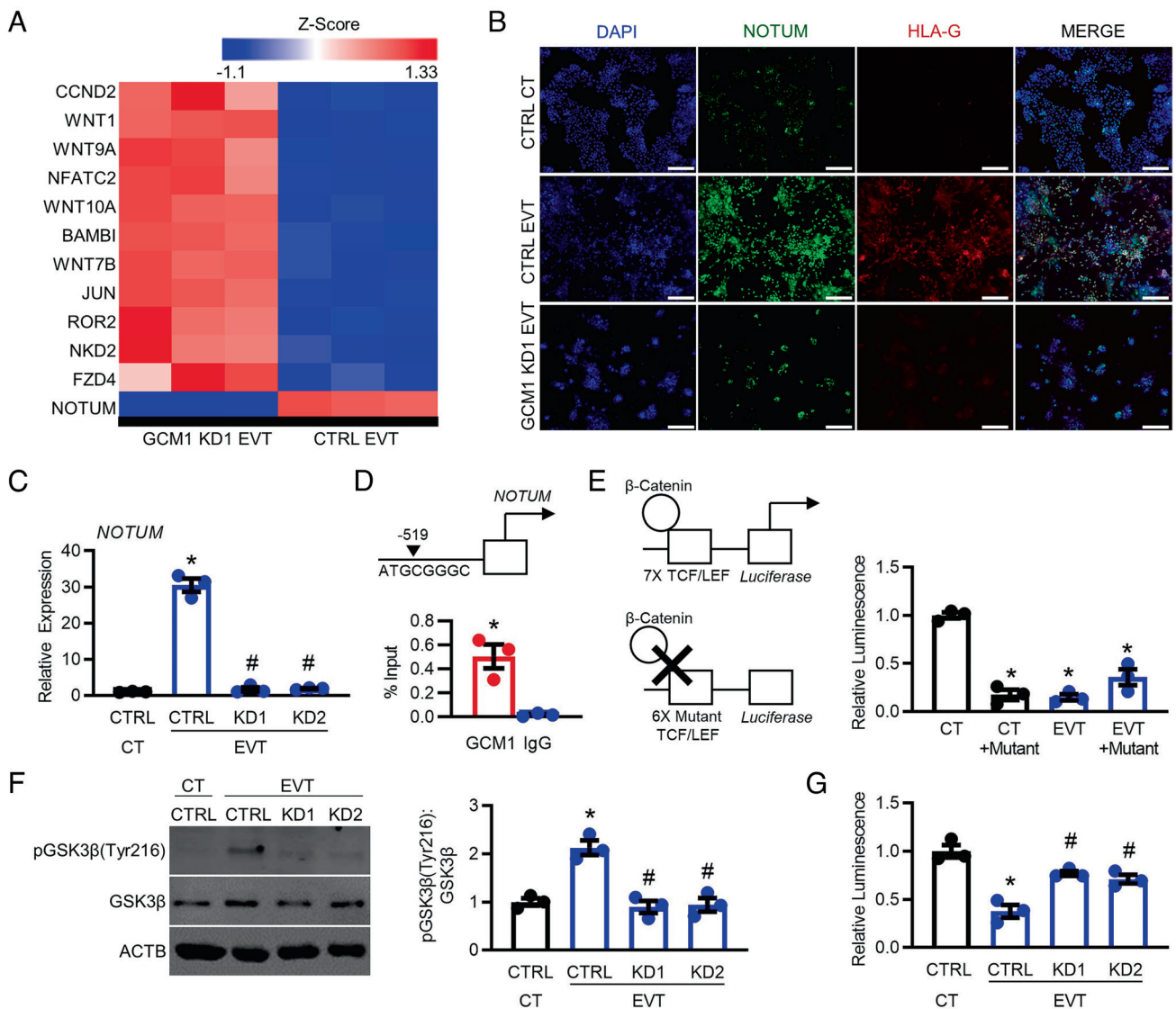


**Fig. 4.** WNT signaling is up-regulated in GCM1-deficient TS cells. (A) Heat map showing Z-score values of Least Squares Means for select genes associated with WNT signaling (path:hsa04310) in control (CTRL) and GCM1 knockdown 1 (KD1) cells cultured in EVT media as determined using RNAseq analysis. Colors represent scaled expression values with blue representing low expression and red showing high expression. (B) Immunofluorescence for NOTUM (green) and HLA-G (red) in CTRL and GCM1 KD1 TS cells differentiated into EVTs. DAPI was used to detect nuclei (blue). (C) Quantitative RT-PCR analysis showing NOTUM expression in CTRL and GCM1 KD1 and KD2 TS cells cultured in EVT media. (D) ChIP was performed for GCM1 or IgG (negative control) in lysates of human TS cells cultured in EVT media for 3 d, followed by quantitative PCR to detect enrichment 519 bp upstream of *NOTUM*. (E) TCF/LEF reporter assay to detect WNT/ $\beta$ -catenin activity in TS cells cultured in CT stem state or in EVT media. Schematics of reporter plasmids can be found to the left of the graph. (F) Western blot analysis of pGSK3 $\beta$ (Tyr216) and total GSK3 $\beta$  in CTRL and GCM1 KD1 and KD2 TS cells cultured in EVT media. ACTB was used as a loading control for Western blotting. (G) TCF/LEF reporter assay showing relative luminescence in CTRL and GCM1 KD1 and KD2 TS cells cultured in EVT media. In (D) and (E), statistical differences are indicated with an asterisk (\*, N = 3, P < 0.05). In (C), (F), and (G), values significantly different between CTRL CT and CTRL EVT are indicated with an asterisk (\*, N = 3, P < 0.05), and values significantly different from CTRL EVT and GCM1 KD EVT are indicated with a number sign (#, N = 3, P < 0.05). (Scale bar, 100  $\mu$ m.)

EVT development. Using in situ hybridization on sections of 7-wk human placenta, we detected strong expression of *NOTUM* in EVT<sub>s</sub> (as demarcated through HLA-G immunohistochemistry; Fig. 5*A*). High expression of *NOTUM* by EVT<sub>s</sub> was also detected using two other human TS cell clones (CT27 and CT29; *SI Appendix*, Fig. S1). We next cultured human TS cells in CT or EVT media in the presence or absence of ABC99, a small molecule inhibitor of NOTUM serine hydrolase activity (26). Cells placed in EVT media in the presence of ABC99 resembled CT<sub>s</sub> and lacked mesenchymal morphology characteristic of human TS cell-derived EVT<sub>s</sub> (Fig. 5*B*). These cells also showed increased expression of *TEAD4* (5.8-fold increase) and decreased expression of *HLA-G* (1.9-fold), *ITGA1* (2.2-fold), and *MMP2* (1.9-fold) when compared with cells placed in EVT media and treated with dimethyl sulfoxide (DMSO, used as a vehicle control; Fig. 5*C*). There was no change in expression of *GCM1* or *ASCL2* between EVT<sub>s</sub> treated with ABC99 or DMSO, indicating that these factors likely work upstream of NOTUM (Fig. 5*C*). Last, to determine whether inhibition of NOTUM is sufficient to maintain WNT/ $\beta$ -catenin activity in cells placed in EVT media, human TS cells were cultured in CT or EVT media and transfected with TCF/LEF *Luciferase* reporters. Similar to our previous observations, differentiation of CT cells into EVT<sub>s</sub> resulted in a 2.5-fold decrease in luminescence (and therefore reduced WNT/ $\beta$ -catenin transcriptional activity). However, when cells were placed in EVT media in the presence of ABC99, luminescence was similar to cells cultured in CT media (Fig. 5*D*). Therefore, our data strongly suggest that *GCM1* promotes EVT differentiation in human TS cells, at least in part, by

inducing NOTUM expression to negatively regulate WNT/ $\beta$ -catenin signaling.

**ASCL2 and NOTUM Restore EVT Differentiation in GCM1-Deficient TS Cells.** Our findings suggest that *GCM1* promotes EVT differentiation by inducing *ASCL2* and NOTUM expression. Therefore, we next sought to determine whether ectopically expressing *ASCL2* and/or NOTUM is sufficient to restore EVT differentiation in *GCM1*-deficient cells. *GCM1* KD1 and KD2 TS cells were placed in EVT differentiation media and after 3 d (the time when *GCM1* levels increase in control cells), plasmids encoding *ASCL2*, NOTUM, or both were transfected into *GCM1*-deficient cells to determine whether EVT differentiation (based on HLA-G levels) and cell invasiveness could be improved. TS cells expressing a control shRNA and transfected with a GFP-expressing plasmid were used in parallel to evaluate the efficiency of EVT differentiation. A schematic of the experimental design is presented in Fig. 6*A*. Transfection efficiency was estimated to be approximately 60% based on the percentage of cells expressing GFP (*SI Appendix*, Fig. S10*A*). As expected, robust expression of *ASCL2* and NOTUM were detectable in *GCM1* KD cells after transfecting plasmids encoding *ASCL2* and NOTUM, respectively. Increased expression of NOTUM did not alter levels of *ASCL2* transcript. Increased expression of *ASCL2*, on the other hand, did appear to increase levels of NOTUM in both *GCM1* KD1 and KD2 cells by approximately three-fold, but this did not reach statistical significance (*SI Appendix*, Fig. S10*B*). Ectopic expression of *ASCL2* increased HLA-G at both mRNA and protein levels in *GCM1*-deficient cells (two-fold increase in HLA-G protein levels in *GCM1* KD cells), whereas addition of NOTUM, or both *ASCL2*

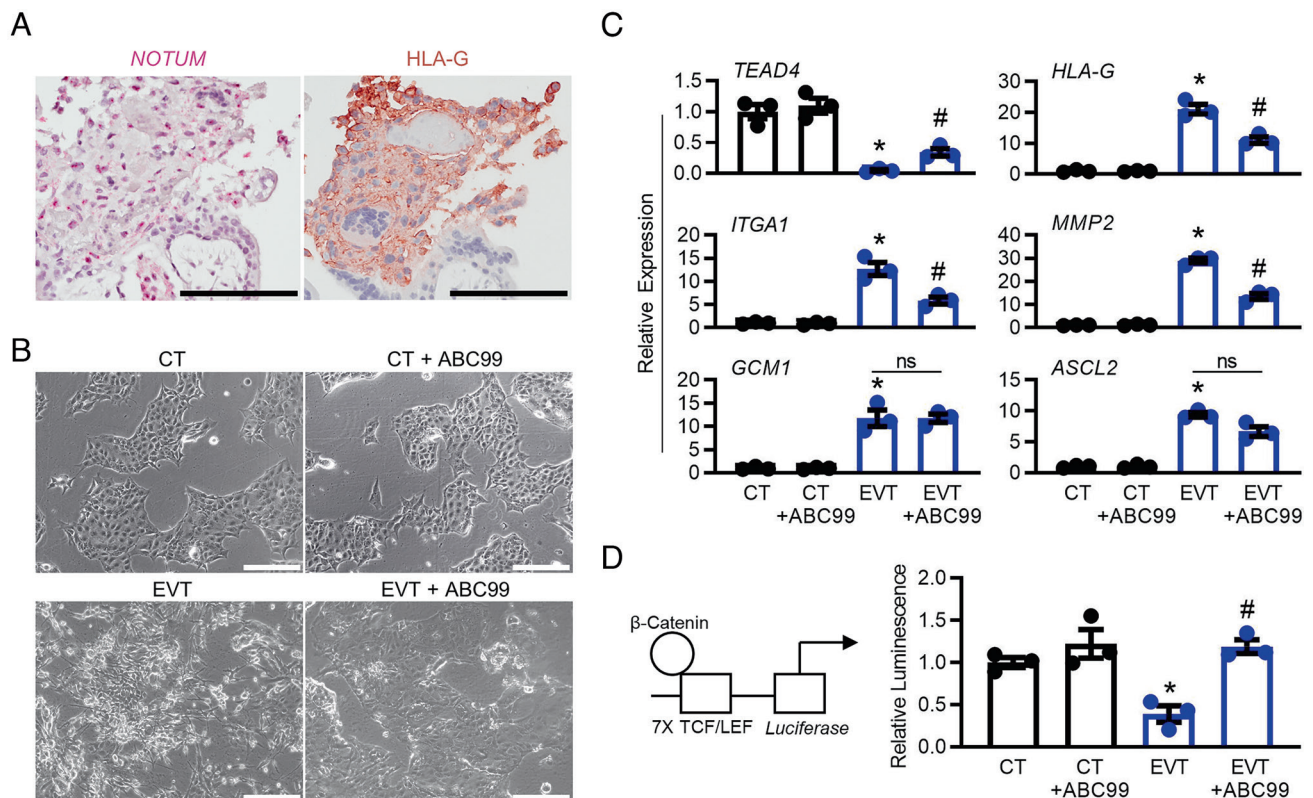


**Fig. 5.** Inhibition of NOTUM leads to increased WNT signaling and poor EVT development. (*A*) In situ hybridization for *NOTUM* (pink dots) and immunohistochemistry for HLA-G (brown) in 7-wk human placenta. (*B*) Phase-contrast images depicting control (DMSO-treated) and ABC99-treated (NOTUM inhibitor; 5 mM) TS cells cultured in CT or EVT media. (*C*) Quantitative RT-PCR analysis showing expression of CT (*TEAD4*) and five EVT markers (*HLA-G*, *ITGA1*, *MMP2*, *GCM1*, and *ASCL2*) in TS cells cultured in CT or EVT media in the presence or absence of ABC99. (*D*) TCF/LEF reporter assay showing relative luminescence in TS cells cultured in CT or EVT media with or without ABC99. Visual of reporter plasmid can be found to the left of the graph. Values significantly different from DMSO-treated CT are indicated with an asterisk (\*,  $N = 3$ ,  $P < 0.05$ ) and values significantly different between DMSO-treated and ABC99-treated cells cultured in EVT media are indicated with a number sign (#,  $N = 3$ ,  $P < 0.05$ ); ns = not statistically significant. (Scale bars, 100  $\mu$ m.)



and NOTUM, increased HLA-G mRNA and protein to levels consistent with control EVT (approximately three-fold increase in HLA-G protein levels in both KD1 and KD2 cells; Fig. 6B and *SI Appendix, Fig. S10B*). HLA-G staining intensity was robust and EVT morphology apparent in GCM1 KD cells transfected with ASCL2, NOTUM, or both ASCL2 and NOTUM (Fig. 6C; only KD1 cells shown). Ectopic expression of ASCL2 and/or NOTUM decreased  $\beta$ -catenin activity (Fig. 6D) and restored the capacity for cells to invade matrix (Fig. 6E). Collectively, our findings show that GCM1 is an essential regulator of human trophoblast differentiation into both ST and EVT pathways, and that GCM1 regulates EVT differentiation by inducing expression of ASCL2 and NOTUM (Fig. 7).

## Discussion

Proper formation of the placenta is vital for healthy human pregnancy and is contingent on the spatiotemporal control of trophoblast differentiation into ST and EVT pathways. In the current study, we identified high expression of the chorion-specific transcription factor GCM1 when human TS cells were directed toward either ST or EVT lineages. GCM1 is classically considered a master regulator of ST formation, a tenet that is consistent with findings from the current study. However, here we also highlight the central role of GCM1 in the formation of EVTs. GCM1 promotes differentiation of human TS cells into EVTs by inducing expression of the EVT master regulator ASCL2 and the WNT antagonist NOTUM. Thus, GCM1 is a multifunctional transcription factor that exerts broad control over human trophoblast differentiation.

In mice, GCM1 is expressed as early as embryonic day 7.5 in clusters of cells within the chorion. By day 9.5, GCM1 expression is restricted to the labyrinth zone, where it works downstream of the transcription factor PPAR $\gamma$  to regulate key genes associated with trophoblast fusion such as *Synb* and *Cebpa* (27–29). Together, these factors promote development of ST layer II (30, 31). The critical role of GCM1 for the development of the placental labyrinth is underscored in mice with reduced levels of this transcription factor. *Gcm1*-heterozygous placentas exhibit increased cell proliferation, poor trophoblast differentiation including reduced *Synb* expression, increased soluble VEGFR1, and placental necrosis. Although *Gcm1*-heterozygous conceptuses are viable, the placental deformities induce preeclampsia-like symptoms in the mother (32). Total ablation of GCM1 results in a severely underdeveloped labyrinth zone and failure of chorioallantoic fusion, resulting in death by embryonic day 10 (33, 34).

An important role for GCM1 in ST formation appears to be conserved in the human placenta (35). GCM1 interacts with other proteins important for trophoblast differentiation, such as p21, DLX3, and CREB/CBP, and promotes expression of numerous genes associated with ST formation, including *ERVW-1* (syncytin 1), *ERVFRD-1* (syncytin 2), *PGF*, *CYP19A1*, and *CKMT1* (36–41). GCM1 also antagonizes  $\Delta$ Np63, which is a key transcription factor contributing to maintenance of the CT stem state (42, 43). Our study supports a central role for GCM1 in human ST formation, since human TS cells with reduced GCM1 expression do not effectively differentiate into ST as shown by the presence of fewer and smaller syncytia as well as decreased expression of ST-related genes (e.g., *ERVFRD-1*, *CGB*, and *HSD11B2*). Furthermore, induced expression of GCM1 caused precocious ST formation, as determined by a higher rate of cell fusion after 3 d of culture in ST differentiation media. Thus, GCM1 promotes ST formation and stability.

Unlike the case in mice, GCM1 is more broadly expressed in the human placenta, being detectable in subsets of both villous trophoblasts and EVTs (12, 40). Although the regulatory role of GCM1 in EVT differentiation has not been well characterized, there is evidence that GCM1 promotes formation of EVTs. For instance,

inhibition of GCM1 in placental explant models decreases outgrowth and invasion of EVTs into Matrigel (13), and ectopic expression of GCM1 in choriocarcinoma cells enhances their invasiveness by inducing expression of the serine peptidase HTRA4 (44). Recent derivation of human TS cells enabled us to mechanistically ascertain the importance of GCM1 for EVT differentiation. We found that induced expression of GCM1 in human TS cells was sufficient to enhance the rate of EVT formation, whereas knockdown of GCM1 hindered EVT differentiation; cells deficient in GCM1 morphologically resembled cells caught in an indeterminate state between CT and EVT, lacked spindle morphology, and had drastically reduced capacity to invade through matrix. RNAseq analysis revealed that numerous genes (e.g., *ADAM19*, *MMP2*, *ITGAI*, *TFPI*) and signaling pathways (e.g., PPAR $\gamma$ ) associated with EVTs were down-regulated in GCM1-deficient cells, whereas other genes (e.g., *TEAD4*) and pathways (Hippo, WNT) were up-regulated, strongly supporting the notion that GCM1 is required for EVT formation.

When placed in media promoting EVT differentiation, one of the most profound gene expression differences between control and GCM1-deficient TS cells was the gene encoding ASCL2. ASCL2 is a transcription factor that promotes differentiation of human EVTs and is a key regulator of junctional zone trophoblast development (analogous to human EVTs) in rodent placentas (16, 22). Knockout of *ASCL2* leads to severe underdevelopment of the junctional zone and embryonic lethality at days 10.5 and 12.5 in mice and rats, respectively (16, 45). We found that GCM1 binds upstream of the gene encoding ASCL2 and similar to the effect of reducing GCM1 expression, knockdown of *ASCL2* in human TS cells leads to abrogated EVT differentiation and consequently, decreased invasion. Tellingly, overexpression of ASCL2 was sufficient to restore EVT differentiation and cellular invasiveness in GCM1-deficient cells, strongly suggesting that *ASCL2* is a downstream target of GCM1 that promotes EVT differentiation. It was recently shown that disrupted expression of *ASCL2* in human TS cells up-regulates transcripts associated with ST, suggesting that ASCL2 may ensure proper formation of EVTs in part by preventing differentiation toward the ST pathway (16). Thus, while GCM1 may be used as a general initiator of human trophoblast differentiation, the lineage trajectory in which cells differentiate may depend on the downstream factors induced by GCM1, and *ASCL2* may be one such factor directing EVT differentiation. Notably, unlike the human placenta where both GCM1 and ASCL2 are detectable in EVT cell columns, GCM1 and ASCL2 expression is confined to the labyrinth zone and junctional zone in the mouse placenta, respectively. Therefore, GCM1 actions on mouse trophoblast differentiation may be more restricted.

Canonical WNT/ $\beta$ -catenin signaling is important for self-renewal of CTs, as shown by hyperactivation of WNT signaling in gestational trophoblastic disease as well as inclusion of GSK3 $\beta$  inhibitors or WNT signaling activators when deriving human TS cells and trophoblast organoids (15, 46–48). Using KEGG pathway analysis, we identified WNT signaling as a major up-regulated pathway in GCM1 knockdown cells cultured in EVT media, indicating that decreased WNT signaling may be needed to initiate EVT differentiation. Our study identified *NOTUM* as a putative target gene directly regulated by GCM1 that may contribute to suppression of WNT signaling during EVT differentiation. NOTUM is a secreted carboxylesterase that mediates O-depalmitoleoylation of WNT proteins, and therefore suppresses WNT signaling (17). The role of NOTUM in the placenta is currently unknown, although strong expression of NOTUM has been detected in human trophoblasts, particularly within floating villi as well as cell columns and invasive EVTs (49, 50). In our study, we did not detect *NOTUM* expression in villous trophoblasts; robust transcript levels were

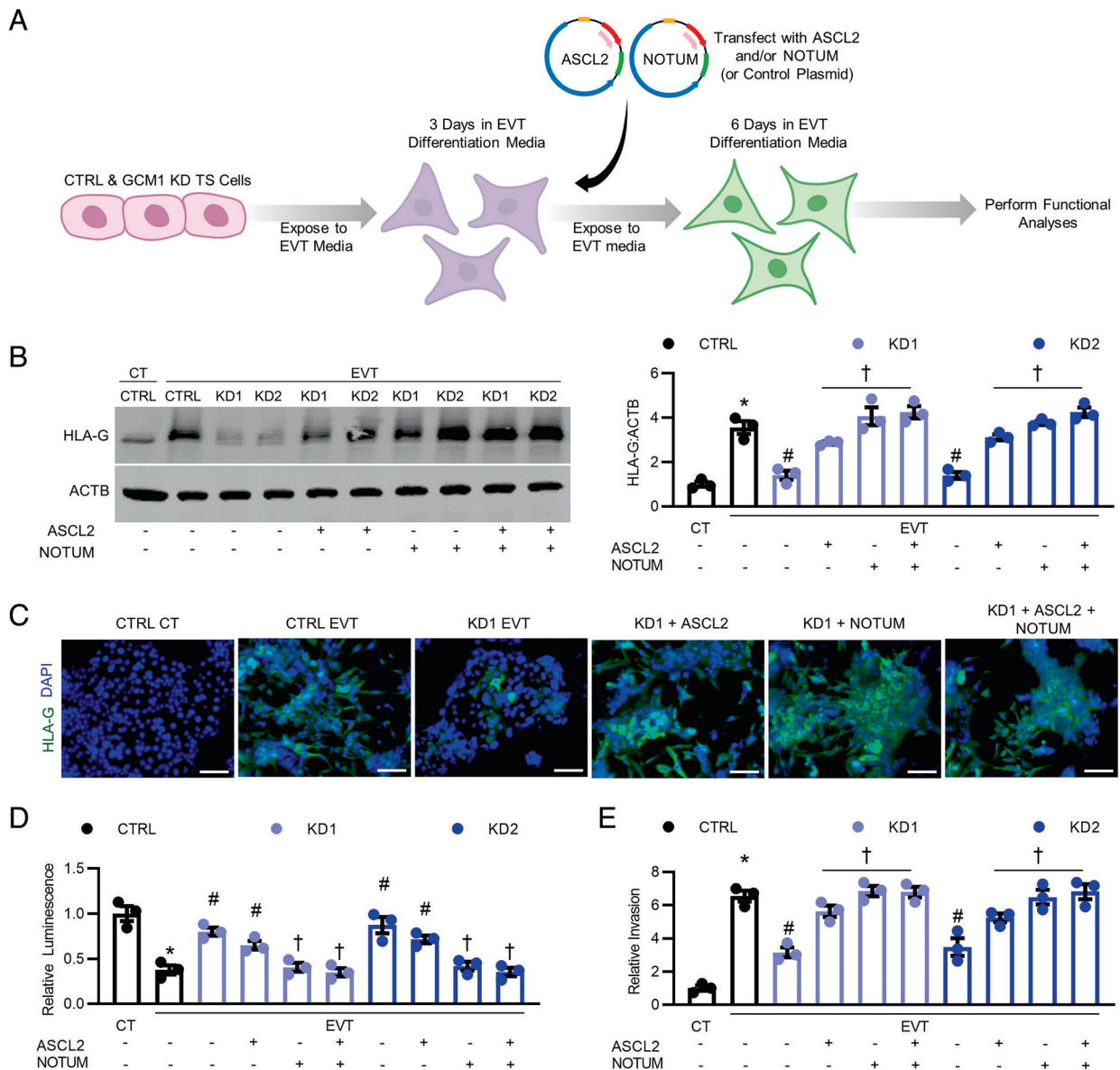


**Fig. 6.** Overexpression of ASCL2 and/or NOTUM in GCM1-deficient cells restores EVT differentiation. (A) Schematic depicting experimental approach. (B) Western blot analysis for HLA-G in control (CTRL) and GCM1 knockdown (KD1 and KD2) TS cells transfected with either control or ASCL2 and/or NOTUM expression plasmids and cultured in EVT differentiation media. ACTB was used as a loading control for Western blotting. (C) Immunofluorescence for HLA-G (green) in CTRL and GCM1 KD1 TS cells cultured in either CT or EVT differentiation media and transfected with either a control plasmid or ASCL2 and/or NOTUM expression plasmids. DAPI was used to demarcate nuclei (blue). Similar results were obtained using GCM1 KD2 cells. (D) TCF/LEF reporter assay showing relative luminescence in CTRL and GCM1 KD1 and KD2 TS cells cultured in CT or EVT media and transfected with either a control plasmid or ASCL2 and/or NOTUM expression plasmids. (E) Relative invasion of CTRL and GCM1 KD1 and KD2 TS cells transfected with either control or ASCL2 and/or NOTUM expression plasmids and cultured in EVT differentiation media. Values significantly different between CTRL CT and CTRL EVT are indicated with an asterisk (\*,  $N = 3$ ,  $P < 0.05$ ); a number sign (#,  $N = 3$ ,  $P < 0.05$ ) denotes values significantly different between CTRL EVT and GCM1 KD EVTs; and a dagger (†,  $N = 3$ ,  $P < 0.05$ ) denotes values significantly different between GCM1 KD EVTs transfected with plasmids encoding ASCL2 and/or NOTUM compared with GCM1 KD EVTs transfected with a control plasmid. (Scale bar, 100  $\mu\text{m}$ .)

observed only within EVTs. We also found that GCM1-deficient human TS cells were unable to up-regulate *NOTUM* expression and maintained high levels of  $\beta$ -catenin activity when placed in EVT differentiation media. This failure to turn off WNT/ $\beta$ -catenin signaling could explain why GCM1 knockdown cells were unable to switch to a differentiated EVT phenotype and resembled undifferentiated CTs. These results were recapitulated by inhibiting NOTUM in human TS cells, resulting in abrogated EVT differentiation and increased  $\beta$ -catenin activity similar to disruption of GCM1 expression. Furthermore, ectopic expression of *NOTUM* (with or without *ASCL2*) was sufficient to rescue EVT differentiation and invasive capacity in GCM1-deficient human TS cells. These results strongly suggest that GCM1 initiates EVT differentiation by directly inducing *NOTUM* expression, resulting in

suppression of WNT/ $\beta$ -catenin signaling. Paradoxically, WNT signaling has been implicated in the promotion of EVT invasiveness (51, 52) indicating that WNT/ $\beta$ -catenin may have a dual role in EVT development similar to other cellular differentiation paradigms (53, 54). The transition between self-renewing CT state and differentiated EVT may require a transient repression of the WNT/ $\beta$ -catenin pathway or switching to distinct coregulators, followed by subsequent reactivation of WNT signaling.

In conclusion, the present study shows that GCM1 is a critical and versatile regulator of human trophoblast differentiation. GCM1 is highly expressed in differentiating EVTs and directly regulates genes vital for EVT differentiation, including *ASCL2* and *NOTUM*. Decreased levels of GCM1 have been reported in pregnancy complications such as preeclampsia, although this is usually

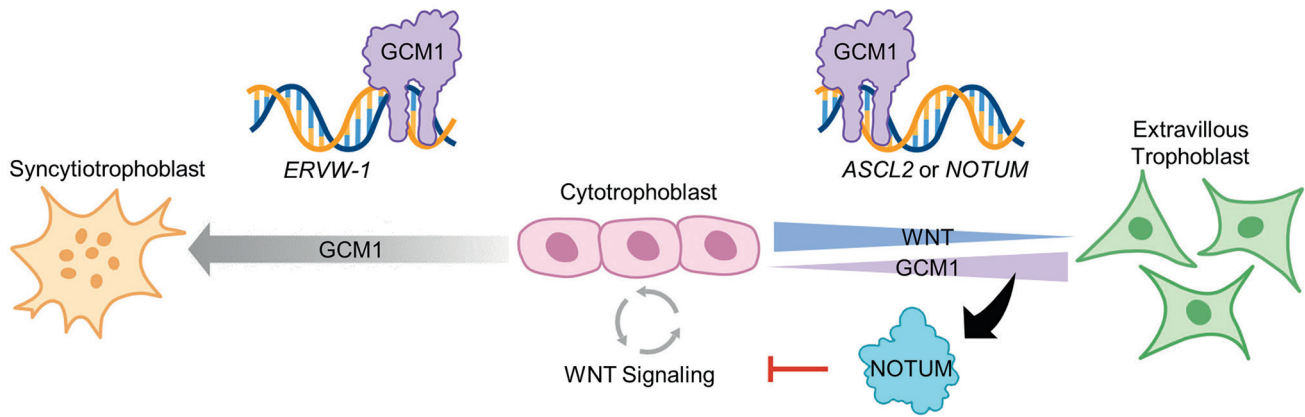


**Fig. 7.** Schematic depicting the role of GCM1 in human trophoblast development.

attributed to defective ST function (55). However, it is possible that reduced GCM1 in these pregnancy complications also hinders EVT differentiation and invasion, which are hallmark features of preeclampsia (8). There are still many unanswered questions for future investigations, such as identification of upstream factors that drive GCM1 expression in differentiating human trophoblasts, discovery of additional genes regulated by GCM1 that promote formation of EVTs, how GCM1 initiates EVT differentiation programs rather than directing cells toward the ST pathway, and the relationship between ASCL2 and NOTUM for directing EVT differentiation. Answers to these and other questions will further our understanding of human EVT formation and may yield clues into the etiology of preeclampsia and other pregnancy complications associated with defective EVT development.

## Materials and Methods

**Tissues, Cells, and Treatments.** Paraffin-embedded tissue sections of 6- and 7-wk human placentas were obtained from the Research Centre for Women's and Children's Health Biobank (RCWIH, Mount Sinai Hospital, Toronto, Canada, <http://biobank.lunenfeld.ca>). All collections were from cesarean deliveries with appropriate consent according to the Declaration of Helsinki. Collections were approved by the Mount Sinai Hospital and the University of Western Ontario research ethics boards.

Human TS cells were maintained as previously described (15). Experiments were performed using the CT30 line, originally derived from a 6-wk-old female placenta. Select experiments were also performed using 7-wk-old placenta-derived CT27 (female) and CT29 (male) lines to ensure findings were consistent among distinct TS cell lines. Undifferentiated TS cells were maintained on cell culture dishes coated with 5  $\mu\text{g}/\text{mL}$  collagen IV (3410-010-02, Bio-Techne, Toronto, ON, Canada). TS cells differentiated toward ST and EVTs were maintained on cell culture dishes coated with 2.5  $\mu\text{g}/\text{mL}$  and 1  $\mu\text{g}/\text{mL}$  collagen IV, respectively. For inducible GCM1 overexpression studies, transduced human TS cells were treated either with cumate (0–300  $\mu\text{g}/\text{mL}$ ; System Biosciences, Palo Alto, CA, USA) to induce expression of GCM1, or an equal volume of PBS as a vehicle control. For NOTUM inhibition studies, human TS cells were treated with ABC99 (5 mM; SML2410, Sigma-Aldrich, Mississauga, ON, Canada), a selective N-hydroxyhydantoin carbamate-based inhibitor of NOTUM serine hydrolase activity, or an equal volume of DMSO as a vehicle control.

Human embryonic kidney (HEK)-293T cells were maintained in DMEM supplemented with 10% FBS, 100 units/mL penicillin, and 100  $\mu\text{M}$  streptomycin. Cells were passaged via light trypsinization prior to reaching confluency and were maintained at 37°C in an atmosphere consisting of 5%  $\text{CO}_2$ . Phase-contrast images of all cells were taken using a Leica DMI1 inverted microscope (Leica Microsystems Inc., Concord, ON, Canada).

**qRT-PCR.** RNA was extracted from cells using RiboZol (Amresco, Mississauga, ON, Canada) according to the manufacturer's instructions, and converted into complementary DNA (cDNA) via reverse transcription (High Capacity cDNA kit, ThermoFisher Scientific, Whitby, ON, Canada). The cDNA was diluted 1:10, then

subjected to qRT-PCR using primers detailed in *S/Appendix, Table S1*. qRT-PCR was performed using a CFX96 Touch (Bio-Rad Laboratories, Mississauga, ON, Canada) and SensiFAST SYBR Lo-ROX PCR Master Mix (BIO98050, FroggaBio, Toronto, ON, Canada). Cycling conditions involved an initial holding step (95°C for 10 min), followed by 40 cycles of two-step PCR (95°C for 15 s and 60°C for 1 min) and a dissociation phase. Relative mRNA expression was calculated using the  $\Delta\Delta\text{Ct}$  method using the geometric means of Ct values obtained using three reference RNAs: *RNA18SN1*, *EEF2*, and *YWHAZ*.

**Western Blotting.** Cell lysates were prepared using radioimmunoprecipitation assay lysis buffer (50 mM Tris, 150 mM NaCl, 1% NP40, 0.5% sodium deoxycholate, 0.1% sodium dodecyl sulfate (SDS)) supplemented with protease inhibitor cocktail (Sigma-Aldrich). A bicinchoninic acid assay (Bio-Rad Laboratories) was used according to the manufacturer's instructions to measure protein concentrations. Approximately 30  $\mu\text{g}$  cell lysate was mixed with 4 $\times$  reducing loading buffer (0.25 M Tris, 8% SDS, 30% glycerol, 0.02% bromophenol blue, and 0.3 M dithiothreitol), boiled for 5 min, and subjected to SDS polyacrylamide gel electrophoresis. Proteins were transferred to a polyvinylidene difluoride membrane and probed using antibodies for HLA-G (21799, 1:1,000, Santa Cruz Biotechnology, Santa Cruz, CA, USA), GCM1 (HPA011343, 1:500, Sigma-Aldrich), ACTB (47778, 1:1,000, Santa Cruz Biotechnology), CGB (1:5,000, PA5-16265, ThermoFisher Scientific), TEAD4 (1:500, HPA056896, Sigma-Aldrich), phosphorylated GSK3 $\beta$ (Tyr216) (1:1,000, NB100-81946, Bio-Techne), or GSK3 $\beta$  (1:1,000, 12456, Cell Signaling Technology, ON, Canada). Membranes were then incubated for 1 h with species-appropriate secondary antibodies, and signals detected using a LI-COR Odyssey imaging system (LI-COR, Lincoln, NE, USA).

**Matrigel-Based Invasion Assay.** Matrigel-based invasion assays were performed as previously described (56). Briefly, transwells (6.5 mm, 8  $\mu\text{m}$  pore, Greiner BioOne, Monroe, NC, USA) were coated with growth factor-reduced Matrigel (400  $\mu\text{g}/\text{mL}$  diluted in the serum-free DMEM/F12 medium; BD Biosciences, Mississauga, ON, Canada) for 3 h. Excess medium was removed prior to plating cells. Approximately  $1 \times 10^5$  cells, retrieved following trypsinization of human TS cells cultured in either the CT or EVT differentiation medium for 6 d, were placed on top of the Matrigel. Each chamber was then placed into a well of a 24-well plate containing either complete CT or EVT culture medium supplemented with 10% FBS and incubated for 24 h at 37°C, 5%  $\text{CO}_2$ . After 24 h, excess cells and Matrigel were discarded from the top of the chamber using a cotton swab, and cells that invaded through to the underside of the transwell were fixed in methanol and stained using Diff-Quik (GE Healthcare). Membranes were placed on slides, and invaded cells counted under a microscope.

**EdU Cell Proliferation Assay.** An EdU incorporation assay (Click-iT EdU Cell Proliferation Assay, ThermoFisher Scientific) was conducted to assess proliferation, as previously described (57). Briefly, 10  $\mu\text{M}$  EdU was added to human TS cell media, and provided to cells for 48 h. Following incubation, TS cells were fixed using 4% paraformaldehyde, permeabilized using 0.3% Triton-X-100, and incubated with Click-iT EdU reaction cocktail for 30 min. Nuclei were stained using Hoechst 33342. Cells were imaged using a Zeiss Axio fluorescence microscope. The percentage of EdU-positive cells was calculated by dividing the number of

EdU-positive nuclei by the total number of nuclei. Results from three random fields of view per well were averaged for each replicate.

**Statistical Analysis.** Statistical analysis for RNAseq can be found in the *SI Appendix*. All other comparisons between two means were tested using Student's *t* test and statistical comparisons between three or more means were tested using ANOVA, followed by Tukey's post hoc test. Means were considered statistically different if *P* was less than 0.05. GraphPad Prism 9.4.0 was used for all graphing and statistical analyses. All experiments were repeated at least three independent times.

**Data, Materials, and Software Availability.** The datasets generated and analyzed in this study have been deposited in the Gene Expression Omnibus (GEO) database, <https://www.ncbi.nlm.nih.gov/geo/> (accession no. [GSE196259](https://www.ncbi.nlm.nih.gov/geo/acc/show/GSE196259)).

**ACKNOWLEDGMENTS.** We would like to thank the donors, RCWIH BioBank, Lunenfeld-Tanenbaum Research Institute, and Mount Sinai Hospital Department of Obstetrics and Gynaecology for placental specimens. We would also like to thank Patrick Lajoie for help generating the inducible *GCM1* expression system, Tunyalux Langsub for illustrative assistance, and the Centre d'expertise

et de services Génome Québec for library preparation and sequencing services. Experiments in this study were supported by the Natural Sciences and Engineering Research Council of Canada (NSERC; 5053), with additional support from the Canadian Institutes of Health Research (PJT152983), both to S.J.R. M.J.J., G.J.B., and R.D.K. are supported by fellowships from the NSERC Alexander Graham Bell Canada and Postgraduate Scholarships-Doctoral Program. A.J. is supported by a Frederick Banting and Charles Best Canada Graduate Scholarship.

Author affiliations: <sup>a</sup>Department of Anatomy and Cell Biology, Schulich School of Medicine and Dentistry, University of Western Ontario, London N6A 5C1, Canada; <sup>b</sup>Robarts Research Institute and Department of Biochemistry, Schulich School of Medicine and Dentistry, University of Western Ontario, London N6A 5C1, Canada; <sup>c</sup>Department of Informative Genetics, Environment and Genome Research Center, Tohoku University Graduate School of Medicine, Sendai 980-8575, Japan; <sup>d</sup>Department of Oncology, Schulich School of Medicine and Dentistry, University of Western Ontario, London N6A 4L6, Canada; <sup>e</sup>London Health Science Center, Lawson Health Research Institute, London N6C 2V5, Canada; and <sup>f</sup>Children's Health Research Institute, Lawson Health Research Institute, London N6C 2V5, Canada

1. M. Y. Turco, A. Moffett, Development of the human placenta. *Development* **146**, 22 (2019).
2. K. J. Baines, S. J. Renaud, Transcription factors that regulate trophoblast development and function. *Prog. Mol. Biol. Transl. Sci.* **145**, 39–88 (2017).
3. A. Jaremek, M. J. Jeyarajah, G. Jaju Bhattad, S. J. Renaud, Omics approaches to study formation and function of human placental syncytiotrophoblast. *Front. Cell Dev. Biol.* **9**, 1543 (2021).
4. S. J. Renaud, M. J. Jeyarajah, How trophoblasts fuse: An in-depth look into placental syncytiotrophoblast formation. *Cell. Mol. Life Sci.* **79**, 433 (2022).
5. J. Pollheimer, S. Vondra, J. Baltayeva, A. G. Berstain, M. Knöfler, Regulation of placental extravillous trophoblasts by the maternal uterine environment. *Front. Immunol.* **9**, 2597 (2018).
6. C. W. Chang, A. K. Wakeland, M. M. Parast, Trophoblast lineage specification, differentiation and their regulation by oxygen tension. *J. Endocrinol.* **236**, R43–R56 (2018).
7. M. J. Soares, K. M. Varberg, K. Iqbal, Hemochorial placentation: Development, function, and adaptations. *Biol. Reprod.* **99**, 196–211 (2018).
8. J. D. Aplin, J. E. Myers, K. Timms, M. Westwood, Tracking placental development in health and disease. *Nat. Rev. Endocrinol.* **16**, 479–494 (2020).
9. M. Hemberger, C. W. Hanna, W. Dean, Mechanisms of early placental development in mouse and humans. *Nat. Rev. Genet.* **21**, 27–43 (2020).
10. L. Woods, V. Perez-Garcia, M. Hemberger, Regulation of placental development and its impact on fetal growth—new insights from mouse models. *Front. Endocrinol.* **9**, 570 (2018).
11. B. Nait-Umesmar, A. B. Copperman, R. A. Lazzarini, Placental expression and chromosomal localization of the human Gcm 1 gene. *J. Histochem. Cytochem.* **48**, 915–922 (2000).
12. D. Baczky *et al.*, Complex patterns of GCM1 mRNA and protein in villous and extravillous trophoblast cells of the human placenta. *Placenta* **25**, 553–559 (2004).
13. D. Baczky *et al.*, Glial cell missing-1 transcription factor is required for the differentiation of the human trophoblast. *Cell Death Differ.* **16**, 719–727 (2009).
14. A. K. Wakeland *et al.*, Hypoxia directs human extravillous trophoblast differentiation in a hypoxia-inducible factor-dependent manner. *Am. J. Pathol.* **187**, 767–780 (2017).
15. H. Okae *et al.*, Derivation of human trophoblast stem cells. *Cell Stem Cell* **22**, 50–63.e6 (2018).
16. K. M. Varberg *et al.*, ASCL2 reciprocally controls key trophoblast lineage decisions during hemochorial placenta development. *Proc. Natl. Acad. Sci. U.S.A.* **118**, e2016517118 (2021).
17. S. Kakugawa *et al.*, Notum deacylates Wnt proteins to suppress signalling activity. *Nature* **519**, 187–192 (2015).
18. R. Vento-Tormo *et al.*, Single-cell reconstruction of the early maternal–fetal interface in humans. *Nature* **563**, 347–353 (2018).
19. M. J. Shannon *et al.*, Cell trajectory modeling identifies a primitive trophoblast state defined by BCAM enrichment. *Development* **149**, dev199840 (2022).
20. F. Y. Lin *et al.*, Dual-specificity phosphatase 23 mediates GCM1 dephosphorylation and activation. *Nucleic Acids Res.* **39**, 848 (2011).
21. C. Dong *et al.*, A genome-wide CRISPR-Cas9 knockout screen identifies essential and growth-restricting genes in human trophoblast stem cells. *Nat. Commun.* **13**, 2548 (2022).
22. A. B. Bogutz *et al.*, Transcription factor ASCL2 is required for development of the glycogen trophoblast cell lineage. *PLoS Genet.* **14**, e1007587 (2018).
23. A. Malassiné *et al.*, Expression of HERV-W Env glycoprotein (syncytin) in the extravillous trophoblast of first trimester human placenta. *Placenta* **26**, 556–562 (2005).
24. M. T. Veeman *et al.*, Zebrafish prickle, a modulator of noncanonical Wnt/Fz signaling, regulates gastrulation movements. *Curr. Biol.* **13**, 680–685 (2003).
25. C. A. Grimes, R. S. Jope, The multifaceted roles of glycogen synthase kinase 3beta in cellular signaling. *Prog. Neurobiol.* **65**, 391–426 (2001).
26. R. M. Suci, A. B. Coggnetta, Z. E. Potter, B. F. Cravatt, Selective irreversible inhibitors of the Wnt-deacylating enzyme NOTUM developed by activity-based protein profiling. *ACS Med. Chem. Lett.* **9**, 563–568 (2018).
27. B. Stecca *et al.*, Gcm1 expression defines three stages of chorio-allantoic interaction during placental development. *Mech. Dev.* **115**, 27–34 (2002).
28. E. Basyuk *et al.*, Murine Gcm1 gene is expressed in a subset of placental trophoblast cells. *Dev. Dyn.* **214**, 303–311 (1999).
29. M. M. Parast *et al.*, PPAR $\gamma$  regulates trophoblast proliferation and promotes labyrinthine trilineage differentiation. *PLoS One* **4**, e8055 (2009).
30. A. Dupressoir *et al.*, A pair of co-opted retroviral envelope syncytin genes is required for formation of the two-layered murine placental syncytiotrophoblast. *Proc. Natl. Acad. Sci. U.S.A.* **108**, E1164–E1173 (2011).
31. D. G. Simmons *et al.*, Early patterning of the chorion leads to the trilaminar trophoblast cell structure in the placental labyrinth. *Development* **135**, 2083–2091 (2008).
32. S. A. Bainbridge *et al.*, Effects of reduced Gcm1 expression on trophoblast morphology, fetoplacental vasculature, and pregnancy outcomes in mice. *Hypertension* **59**, 732–739 (2012).
33. L. Anson-Cartwright *et al.*, The glial cells missing-1 protein is essential for branching morphogenesis in the chorioallantoic placenta. *Nat. Genet.* **25**, 311–314 (2000).
34. J. Schreiber *et al.*, Placental failure in mice lacking the mammalian homolog of glial cells missing, GCMa. *Mol. Cell. Biol.* **20**, 2466–2474 (2000).
35. F. Söncin, D. Natale, M. M. Parast, Signaling pathways in mouse and human trophoblast differentiation: A comparative review. *Cell. Mol. Life Sci.* **72**, 1291 (2015).
36. C. Yu *et al.*, GCMa regulates the syncytin-mediated trophoblastic fusion. *J. Biol. Chem.* **277**, 50062–50068 (2002).
37. C.-Y. Liang *et al.*, GCM1 regulation of the expression of syncytin 2 and its cognate receptor MFSD2A in human placenta. *Biol. Reprod.* **83**, 387–395 (2010).
38. Y. H. Chiu *et al.*, New insights into the regulation of placental growth factor gene expression by the transcription factors GCM1 and DLX3 in human placenta. *J. Biol. Chem.* **293**, 9801–9811 (2018).
39. K. Yamada, H. Ogawal, S. I. Honda, N. Harada, T. Okazaki, A GCM motif protein is involved in placenta-specific expression of human aromatase gene. *J. Biol. Chem.* **274**, 32279–32286 (1999).
40. X. Lu *et al.*, Fine-tuned and cell-cycle-restricted expression of fusogenic protein syncytin-2 maintains functional placental syncytia. *Cell Rep.* **21**, 1150–1159 (2017).
41. S. Li, M. S. Roberson, DLX3 interacts with GCM1 and inhibits its transactivation-stimulating activity in a homeodomain-dependent manner in human trophoblast-derived cells. *Sci. Rep.* **7**, 1–13 (2017).
42. Y. Li *et al.*, BMP4-directed trophoblast differentiation of human embryonic stem cells is mediated through a  $\Delta$ Np63+ cytotrophoblast stem cell state. *Development* **140**, 3965–3976 (2013).
43. L. J. Wang *et al.*, Functional antagonism between  $\Delta$ Np63 $\alpha$  and GCM1 regulates human trophoblast stemness and differentiation. *Nat. Commun.* **13**, 1–16 (2022).
44. L. J. Wang, M. L. Cheong, Y. S. Lee, M. T. Lee, H. Chen, High-temperature requirement protein A4 (HtrA4) suppresses the fusogenic activity of syncytin-1 and promotes trophoblast invasion. *Mol. Cell. Biol.* **32**, 3707 (2012).
45. M. Tanaka *et al.*, Parental origin-specific expression of Mash2 is established at the time of implantation with its imprinting mechanism highly resistant to genome-wide demethylation. *Mech. Dev.* **87**, 129–142 (1999).
46. S. Haider *et al.*, Self-renewing trophoblast organoids recapitulate the developmental program of the early human placenta. *Stem Cell Rep.* **11**, 537–551 (2018).
47. M. Y. Turco *et al.*, Trophoblast organoids as a model for maternal–fetal interactions during human placentation. *Nature* **564**, 263–281 (2018).
48. Z. Zhang *et al.*, Wnt/ $\beta$ -catenin signaling pathway in trophoblasts and abnormal activation in preeclampsia. *Mol. Med. Rep.* **16**, 1007–1013 (2017).
49. J. F. Robinson *et al.*, Transcriptional dynamics of cultured human villous cytotrophoblasts. *Endocrinology* **158**, 1581 (2017).
50. S. Haider *et al.*, Transforming growth factor- $\beta$  signaling governs the differentiation program of extravillous trophoblasts in the developing human placenta. *Proc. Natl. Acad. Sci. U.S.A.* **119**, e2120667119 (2022).
51. M. Knöfler *et al.*, Human placenta and trophoblast development: Key molecular mechanisms and model systems. *Cell. Mol. Life Sci.* **76**, 3479–3496 (2019).
52. H. Takahashi *et al.*, Extravillous trophoblast invasion accelerated by WNT3A, 5A, and 10B via CD44. *J. Matern. Fetal. Neonatal Med.* **34**, 3377–3385 (2021).
53. J. L. Teo, M. Kahn, The Wnt signaling pathway in cellular proliferation and differentiation: A tale of two coactivators. *Adv. Drug Deliv. Rev.* **62**, 1149–1155 (2010).
54. A. Ring, Y. M. Kim, M. Kahn, Wnt/ $\beta$ -catenin signaling in adult stem cell physiology and disease. *Stem Cell Rev.* **10**, 512 (2014).
55. B. Armistead *et al.*, Induction of the PPAR $\gamma$  (peroxisome proliferator-activated receptor  $\gamma$ )-GCM1 (glial cell missing 1) syncytialization axis reduces sFLT1 (soluble fms-like tyrosine kinase 1) in the preeclamptic placenta. *Hypertens* **78**, 230–240 (2021).
56. M. J. Jeyarajah, G. Jaju Bhattad, B. F. Kops, S. J. Renaud, Syndecan-4 regulates extravillous trophoblast migration by coordinating protein kinase C activation. *Sci. Rep.* **9**, 10175 (2019).
57. M. J. Jeyarajah, G. Jaju Bhattad, D. M. Hillier, S. J. Renaud, The transcription factor OVOL2 represses ID2 and drives differentiation of trophoblast stem cells and placental development in mice. *Cells* **9**, 840 (2020).